

# Lanthanum-Doped Zinc Oxide Thin Films: A Study on Optoelectronic Properties <sup>†</sup>

Ayesha Tabriz <sup>1</sup>, Nadia Shahzad <sup>1,\*</sup>, Saad Nadeem <sup>1</sup>, Sana Mehmood <sup>1</sup>, Naseem Iqbal <sup>1</sup>, Ghulam Ali <sup>1</sup>  
and Muhammad Imran Shahzad <sup>2</sup>

<sup>1</sup> U.S.-Pakistan Centre for Advanced Studies in Energy (USPCAS-E), National University of Sciences and Technology (NUST), H-12 Sector, Islamabad 44000, Pakistan; ash.tab96@yahoo.com (A.T.); shk\_saadi@outlook.com (S.N.); sanamehmood509@gmail.com (S.M.); naseem@uspcase.nust.edu.pk (N.I.); ali@uspcase.nust.edu.pk (G.A.)

<sup>2</sup> Nanosciences and Technology Department (NS&TD), National Centre for Physics (NCP), Islamabad 44000, Pakistan; imran-shahzad@live.com

\* Correspondence: nadia@uspcase.nust.edu.pk

<sup>†</sup> Presented at the 6th Conference on Emerging Materials and Processes (CEMP 2023), Islamabad, Pakistan, 22–23 November 2023.

**Abstract:** To enhance the overall performance of perovskite solar cells, the quality of the electron transport layer (ETL) held significant importance. Zinc oxide (ZnO) emerged as highly promising due to its exceptional optical and electrical characteristics. This study included the incorporation of lanthanum (La III) into the ZnO lattice to improve its optoelectronic properties. All the produced thin films were crystallized at low annealing temperatures. Through careful analysis, it was observed that the inclusion of doping with 4% La (III) resulted in increased crystallinity, leading to low surface roughness. Additionally, this doping strategy facilitated enhanced mobility of charge carriers and conductivity.

**Keywords:** rare earth element; thin films; elemental doping; electron transport layer



**Citation:** Tabriz, A.; Shahzad, N.; Nadeem, S.; Mehmood, S.; Iqbal, N.; Ali, G.; Shahzad, M.I. Lanthanum-Doped Zinc Oxide Thin Films: A Study on Optoelectronic Properties. *Mater. Proc.* **2024**, *17*, 9. <https://doi.org/10.3390/materproc2024017009>

Academic Editors: Sofia Javed, Waheed Miran, Erum Pervaiz and Iftikhar Ahmad

Published: 9 April 2024



**Copyright:** © 2024 by the authors. Licensee MDPI, Basel, Switzerland. This article is an open access article distributed under the terms and conditions of the Creative Commons Attribution (CC BY) license (<https://creativecommons.org/licenses/by/4.0/>).

## 1. Introduction

ZnO is an interesting optoelectronic material with direct band gap energy (3.37 eV), a wurtzite structure with optical transparency in the visible range, low toxicity and a large exciton binding energy (60 meV) at room temperature [1]. However, zinc oxide has some limitations that restrict its use. The high energy gap, limited absorption of visible light rays and low electrical conductivity of ZnO limit its uses in electronics, super-capacitors and solar energy applications. One of the effective strategies for solving these limitations is the doping process. The effect of many metal dopants on the physical, structural, optical and electrical properties of zinc oxide were observed. In last few years, rare earth metals such as La, Ce, Dy, Sm, Nd and Gd have gained a lot of attention as they can significantly improve the electrical and optical properties of the main structure. Rare earth elements are also known to be laser active when inserted into an amorphous or crystalline structure to obtain IR radiation [2,3]. They can also alter the electrical, optical and structural properties of the thin films by doping with the appropriate type and concentrations [4,5]. Nanostructures and thin films of ZnO have been obtained by different methodologies such as RF sputtering, the sol-gel process (SG), pulsed laser deposition (PLD), spin coating (SP), chemical vapor deposition (CVD) and spray pyrolysis (SP).

Lanthanum is a rare earth element with a wide energy band gap, electronic configuration of [Xe] 5d1 6s2 and a large spectral area; in addition, the 4f–4f intra-shell transitions in La give very strong emission peaks in the visible and near-IR regions [4,6]. La can reduce the recombination of photo-generated electron-hole pairs by trapping the electrons and hence, enhance the photocatalytic activity of ZnO [7].

In the literature, very few research papers exist on La-doped ZnO thin films prepared via the spin coating method [2]. This paper is therefore devoted to sol-gel spin-coated La-doped ZnO thin films (pure ZnO, 3%, 4%, 5% La-doped ZnO). We have discussed the experimental results along with some evaluations related to their structural, optical and electrical properties.

## 2. Materials and Methods

Zinc acetate dihydrate (CAS No. 5970-45-6), La (III) chloride heptahydrate (CAS No. 10025-84-0), 2-methoxyethanol (CAS No. 109-86-4), diethanolamine (CAS No. 111-42-2) and Fluorine-doped Tin Oxide (FTO) glass substrates were purchased from Sigma-Aldrich (St. Louis, MO, USA). All the chemicals were used directly without further purification.

The precursor solutions for pure and La-doped ZnO thin films,  $\text{La}_x\text{Zn}_{1-x}\text{O}$  ( $x = 0.0, 3.0, 4.0$  and  $5.0\%$ ) were prepared using the sol-gel method. In this process, a 0.5 M Zn precursor solution was prepared by dissolving zinc acetate  $[\text{Zn}(\text{CH}_3\text{CO}_2)_2 \cdot 2\text{H}_2\text{O}]$  (ZnAc) in 2-methoxyethanol (solvent) and diethanolamine (DEA,  $\text{C}_4\text{H}_{11}\text{NO}_2$ ) and stirred at  $50\text{--}60\text{ }^\circ\text{C}$  until the solution became clear. DEA was used as a stabilizer to increase the solubility. The 0.5 M La precursor solution was prepared by dissolving lanthanum (III) chloride heptahydrate ( $\text{LaCl}_3 \cdot 7\text{H}_2\text{O}$ ) in ethanol (solvent) and stirring at room temperature for 30 min. La-doped ZnO samples (3%, 4% and 5%) were prepared by simply dissolving two precursor solutions in appropriate concentrations. The FTO glass substrates were sonicated in ethanol, acetone and propanol for 15 min each. After drying, all the samples were plasma cleaned before spin coating. The precursor solution was deposited onto the substrate at 3000 rpm for 30 s using a spin coater. After spin coating, the films were treated at  $150\text{ }^\circ\text{C}$  for 10 min on a hot plate to vaporize the solvent and to eliminate volatile organic residuals. Then, thin films were annealed on the hot plate at  $300\text{ }^\circ\text{C}$  for 1 h.

## 3. Results and Discussions

### 3.1. Structural Properties

Figure 1a shows the XRD patterns of all the deposited films on glass slides, pure ZnO and La-doped ZnO (3%, 4% and 5%). All the peak positions matched with previously reported data in the literature [8,9]. It was observed that all the films show crystalline structures attributed to the hexagonal wurtzite ZnO. No additional phases linked to metallic Zn, La or La compounds were seen, even at the highest doping level of 5%. All the peaks became sharp when La was added up to a concentration of 4%. After that, a sudden decrease in peak size was observed because the ionic radius of Zn (0.074 nm) is smaller than that of La (0.119 nm); hence, further addition of La results in a small lattice distortion and affects the internal micro-strain of the ZnO structure. Figure 1b shows the peak (100) shifting towards lower  $2\theta$ , which indicates the successful integration of La atoms in the ZnO lattice, and La additions did not change the hexagonal structure of the ZnO films. No additional peak confirms that the precursors were completely transformed into the ZnO phase [8].

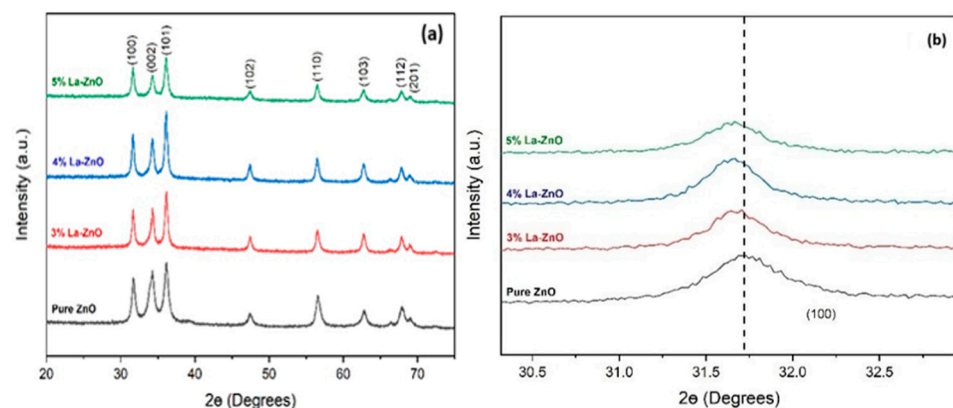


**Figure 1.** (a) XRD patterns of pure ZnO and La-doped ZnO and (b) the (100) peak shift to lower  $2\theta$  values.

### 3.2. Optical Properties

In Figure 2a, the optical transmittance spectra of pure ZnO and La-doped ZnO films with different La contents are presented. It is observed that all films exhibited high transparency of more than 85% in the visible region of 400–800 nm. In Figure 2b, the  $E_g$  values were calculated by extrapolating the linear part of the plot of  $(\alpha h\nu)^2$ . The  $E_g$  value for the pure ZnO film was 3.30 eV; by incorporating La, the  $E_g$  value increased to 3.32 eV with 4% La. Further doping decreased the  $E_g$ . The broadening of the band gap with increasing La content in the ZnO lattice is due to the substitution of  $Zn^{2+}$  ions with  $La^{3+}$  ions. In the undoped ZnO sample, the ionic bond between  $Zn^{2+}$  and  $O^{2-}$  results in the absence of free carrier charges. By replacing  $Zn^{2+}$  ions with  $La^{3+}$  ions in the ZnO lattice, extra free electrons are incorporated into the valence band. Given that the lowest states in the conduction band are occupied by electrons, an additional energy input is required for electrons in the valence band to move into the empty states in the conduction band. Based on this reason, a continuous increase in  $E_g$  values with rising  $La^{3+}$  content is possible due to the higher electron density in the films. However,  $E_g$  values reduced at the 5% La doping level because crystal defects formed in the ZnO lattice [10]. The results are also confirmed by XRD data.

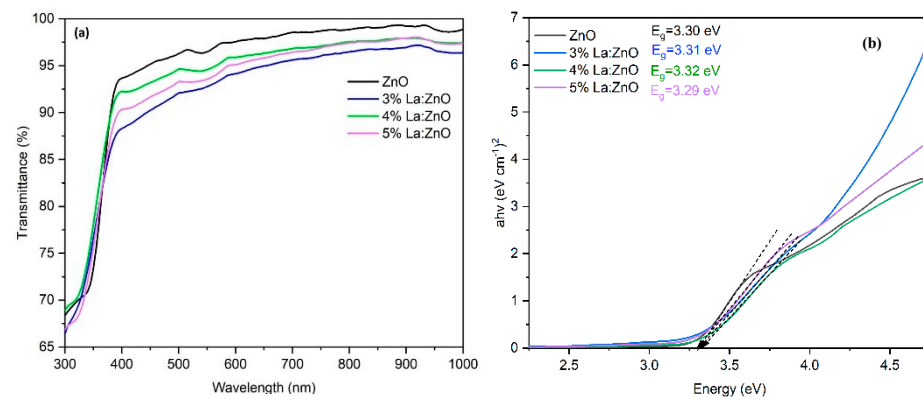


**Figure 2.** (a) The optical transmittance spectrum ( $T$  %) vs. wavelength and (b) Tauc plot of pure ZnO and (3%, 4% and 5%) La-doped ZnO films.

### 3.3. Electrical Properties

In Table 1, mobility and conductivity of pure ZnO and (3%, 4% and 5%) La-doped ZnO films are tabulated. These data were provided by the Hall effect measurement. Pure ZnO showed the least mobility and conductivity  $22.3 \text{ cm}^3 \cdot \text{V}^{-1} \cdot \text{s}^{-1}$  and  $1.26 \times 10^2 (\Omega \cdot \text{cm})^{-1}$ , respectively, while these parameters increased substantially with the incorporation of La doping up until a concentration of 4%. The increase in conductivity is due to the improvement in charge carrier mobility and surface smoothness. After 4% La doping in ZnO, both mobility and conductivity decrease due to microstructure distortion, defects and strain [11].

**Table 1.** Mobility and conductivity of pure Zn and La-doped ZnO films.

ETL Composition	Mobility ( $\times 10^1 \text{ cm}^3 \cdot \text{V}^{-1} \cdot \text{s}^{-1}$ )	Conductivity ( $\times 10^2 \Omega \cdot \text{cm})^{-1}$ )
ZnO	2.23	1.26
3% La:ZnO	4.02	3.94
4% La:ZnO	6.35	5.22
5% La:ZnO	3.48	2.53

### 3.4. Hydrophilic Properties

Contact angle analysis helps to find the hydrophilic nature and wettability of the film. Geometrically, the contact angle is the angle of a liquid drop at the three-phase boundary intersection between a solid, liquid and gas. The wettability of the film depends on its

surface free energy, chemical composition, microstructures and surface topography. A total of 0.5  $\mu\text{L}$  water was dropped onto the thin film surface using a microsyringe. Figure 3 shows the images of the contact angles; the obtained values were  $31^\circ$ ,  $28^\circ$ ,  $20.20^\circ$  and  $27.60^\circ$  for ZnO, 3% and 4% and 5% for La-(III)-doped ZnO. It was observed that the contact angles for 3%, 4% and 5% La-doped ZnO samples were lower as compared to pure ZnO. The results could be ascribed to the crystallinity and microstructural changes after doping. The decreased contact angle refers to a lower surface energy, reduced surface roughness, and improved nucleation and growth of the film [9].

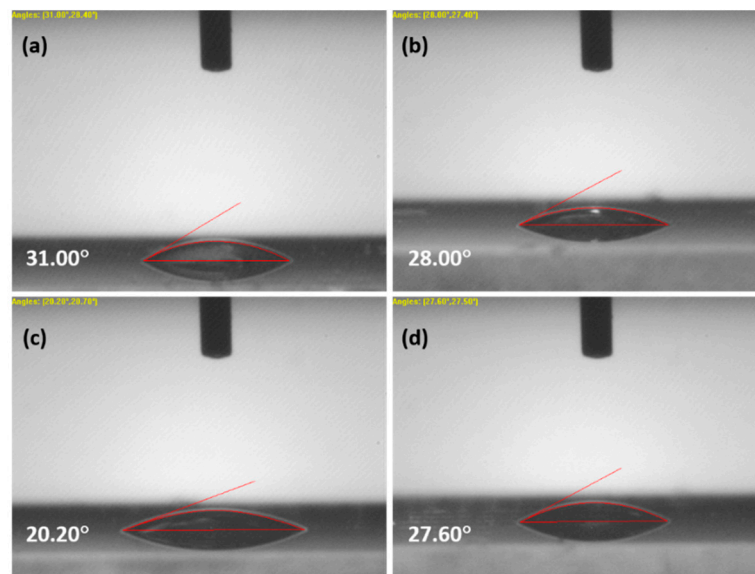


**Figure 3.** Contact angle images for (a) ZnO, and (b) 3%, (c) 4%, (d) 5% La-doped ZnO.

#### 4. Conclusions

In this study, we have investigated the effect of La doping on the optical, electrical and structural properties of ZnO films. All the films showed crystalline structures attributed to the hexagonal wurtzite. XRD peaks of (100), (002) and (101) became sharp by increasing La doping up to a concentration of 4%. After that, further doping caused a reduction due to the small lattice distortion and internal micro-strain in the ZnO structure. Band gap energy reaches a maximum and surface roughness is at the minimum at a 4% concentration. The improved structural, electrical and optical properties of La-doped ZnO make it a good candidate as an ETL material for PCS application.

**Author Contributions:** Conceptualization, A.T., S.M. and S.N.; methodology, A.T.; software, S.M. and S.N.; validation, N.S., M.I.S. and N.I.; formal analysis, G.A.; investigation, A.T.; resources, N.S.; writing—original draft preparation, A.T.; writing—review and editing, A.T., S.N. and S.M.; supervision, N.S. All authors have read and agreed to the published version of the manuscript.

**Funding:** This research received no external funding.

**Institutional Review Board Statement:** Not Applicable.

**Informed Consent Statement:** Not Applicable.

**Data Availability Statement:** The data presented in this study are available on request from the corresponding author.

**Acknowledgments:** We would like to extend our sincere gratitude to Saqib Ali and lab engineers Nisar and Naveed for their invaluable assistance with the characterization tools used in this study.

**Conflicts of Interest:** The authors declare no conflict of interest.

## References

1. Gupta, T.K. Application of zinc oxide varistors. *J. Am. Ceram. Soc.* **1990**, *73*, 1817–1840. [[CrossRef](#)]
2. Chen, J.; Wang, J.; Zhang, F.; Zhang, G.; Wu, Z.; Yan, P. The effect of La doping concentration on the properties of zinc oxide films prepared by the sol–gel method. *J. Cryst. Growth* **2008**, *310*, 2627–2632. [[CrossRef](#)]
3. Avram, D.; Gheorghe, C.; Rotaru, C.; Cojocaru, B.; Florea, M.; Parvulescu, V.; Tiseanu, C. Lanthanide–lanthanide and lanthanide–defect interactions in co-doped ceria revealed by luminescence spectroscopy. *J. Alloys Compd.* **2014**, *616*, 535–541. [[CrossRef](#)]
4. Iwan, S.; Zhao, J.; Tan, S.; Bambang, S.; Hikam, M.; Fan, H.; Sun, X. Ion-dependent electroluminescence from trivalent rare-earth doped n-ZnO/p-Si heterostructured light-emitting diodes. *Mater. Sci. Semicond. Process.* **2015**, *30*, 263–266. [[CrossRef](#)]
5. Jia, T.; Wang, W.; Long, F.; Fu, Z.; Wang, H.; Zhang, Q. Fabrication, characterization and photocatalytic activity of La-doped ZnO nanowires. *J. Alloys Compd.* **2009**, *484*, 410–415. [[CrossRef](#)]
6. Zamiri, R.; Lemos, A.; Reblo, A.; Ahangar, H.A.; Ferreira, J. Effects of rare-earth (Er, La and Yb) doping on morphology and structure properties of ZnO nanostructures prepared by wet chemical method. *Ceram. Int.* **2014**, *40*, 523–529. [[CrossRef](#)]
7. Anandan, S.; Vinu, A.; Mori, T.; Gokulakrishnan, N.; Srinivasu, P.; Murugesan, V.; Ariga, K. Photocatalytic degradation of 2, 4, 6-trichlorophenol using lanthanum doped ZnO in aqueous suspension. *Catal. Commun.* **2007**, *8*, 1377–1382. [[CrossRef](#)]
8. Abdel-Latif, M.K.; Mobarak, M.; Revaprasadu, N.; Ashraf, A.H.; Othman, W.; Khalefa, M.M.; Aboud, A.A.; Ismail, M. Effect of doping on the structural, optical and electrical properties of La-doped ZnO thin films. *J. Mater. Sci. Mater. Electron.* **2023**, *34*, 254. [[CrossRef](#)]
9. Ilkhechi, N.N.; Ghobadi, N.; Yahyavi, F. Enhanced optical and hydrophilic properties of V and La co-doped ZnO thin films. *Opt. Quantum Electron.* **2017**, *49*, 39. [[CrossRef](#)]
10. Ahmed, M.M.; Tawfik, W.Z.; Elfayoumi, M.; Abdel-Hafiez, M.; El-Dek, S. Tailoring the optical and physical properties of La doped ZnO nanostructured thin films. *J. Alloys Compd.* **2019**, *791*, 586–592. [[CrossRef](#)]
11. Aal, N.A.; Al-Hazmi, F.; Al-Ghamdi, A.A.; Hendi, A.; Alorainy, R.; Nawar, A.; El-Gazzar, S.; El-Tantawy, F.; Yakuphanoglu, F. Nanostructure lanthanum doped zinc oxide optical materials. *J. Nanoelectron. Optoelectron.* **2014**, *9*, 624–634. [[CrossRef](#)]

**Disclaimer/Publisher’s Note:** The statements, opinions and data contained in all publications are solely those of the individual author(s) and contributor(s) and not of MDPI and/or the editor(s). MDPI and/or the editor(s) disclaim responsibility for any injury to people or property resulting from any ideas, methods, instructions or products referred to in the content.